Open Access

SCHOLARENA

SAJ Biotechnology

RESEARCH ARTICLE

ISSN: 2375-6713

Dissipative Effects in Nuclear Fission Studied with Kinematically Complete Measurements

Rodríguez-Sánchez JL[1,2,*]

[1]*Universidad de Santiago de Compostela, E-15782 Santiago de Compostela, Spain*
[2]*GSI, Helmholtz Center for Heavy Ion Research GmbH, D-64291 Darmstadt, Germany*

[*]**Corresponding author:** Rodríguez-Sánchez JL, Universidad de Santiago de Compostela, E-15782 Santiago de Compostela, Spain, Tel: 34 881 811 000, E-mail: joseluis.rodriguez.sanchez@usc.es

Citation: Rodríguez-Sánchez JL (2018) Dissipative Effects in Nuclear Fission Studied with Kinematically Complete Measurements. SAJ Biotech 5: 204

Article history: Received: 04 April 2018, **Accepted:** 29 May 2018, **Published:** 31 May 2018

Abstract

Nuclear fission dynamic is investigated using spallation reactions induced by protons on ^{208}Pb. This reaction allows to produce fissioning systems with low angular momentum, small deformations, and high excitation energies that enhance the dissipative effects in fission. Kinematically complete measurements of fission fragments and light-charged particles emitted in coincidence were performed by the use of the SOFIA setup combined with the inverse kinematics technique, allowing for the first time a full identification in atomic and mass number of the two fission fragments. These measurements permit to define new fission observables for the investigation of temperature and deformation dependencies of the dissipation parameter. In addition, these new measurements are also interesting for technical applications, such as accelerator-driven systems (ADS), radioprotection in space, and shielding at accelerators.

Keywords: Nuclear Fission; Spallation Reactions

Introduction

Fission is the clearest example of large-scale collective excitations in nuclei. Since its discovery, the progress in the understanding of the fission process has been driven by new experimental results. In particular, the investigation of pre- and postscission neutron multiplicities, giant dipole resonance (GDR) γ-ray emission, multiplicities of charged particles, fission and evaporation cross sections established that the dynamical evolution of the fissioning system cannot be explained just in terms of the statistical model of Bohr and Wheeler [1-6]. These results suggested that the under-standing of the fission process requires a dynamical approach, describing the coupling of intrinsic and collective excitations of the nuclear constituents. Here, the transfer of energy between the intrinsic and collective excitations is governed by dissipation due to fluctuating forces. In this context, transport models based on the Fokker-Planck or the Langevin equations have proven to be a suitable tool [7-8].

However, the dynamics of fission is still far from being fully understood because our theoretical and experimental knowledge is not yet complete. Several works claim that the reduced dissipation parameter (β), defined according to Ref. [7], could change with the nuclear deformation or with the nuclear temperature [8]. These ideas are still under debate because they could be biased by experimental conditions [9].

The ground-to-saddle dynamics and more particularly the presence of transient time, which corresponds to the time required to reach 90% of the stationary fission flux across the barrier, has been actively debated during the last decade [3,5,9,10]. Experiments taking advantage of spallation and fragmentation induced fission reactions brought some light into the problem [9,11]. The combined use of the inverse kinematics technique and an efficient detection setup made it possible to identify fission reactions and determine the atomic number of the final fission fragments very accurately. The sum of the charges of both fission fragments was used as a measurement of the initial excitation energy, while partial fission cross sections and the width of the charge distribution of the fission fragments were shown to be sensitive to presaddle dynamical effects [9-16]. The measurements obtained for many different fissioning systems over a broad range in fissility and temperature were compatible with a constant value of the reduced dissipation parameter at small deformations of $\beta = 4.5 \times 10^{21}$ s^{-1}, corresponding to transient times between 1.0 and 3.3×10^{-21} s. These results are compatible with the ones obtained from the investigation of some fusion reactions [9,17]. Moreover, the overall good description of the data over a broad range of excitation energies also validated previous conclusions on the temperature independence of the dissipation parameter [4,9,10,18].

Postsaddle dissipative effects have been mostly investigated by measuring prescission particles and γ-rays emitted in fusion-fission reactions [8,19,20]. In some cases, fission or evaporation-residue cross sections were also measured, constraining presaddle effects. Because of the different saddle-to-scission deformations lengths reached in these reactions, pre- and postsaddle dissipative effects were enhanced by investigating low and high fissility systems, respectively. Most of the results obtained in these works seem compatible with presaddle reduced dissipation parameters between 2 and 6 × 10^{21} s^{-1}, while the saddle-to-scission dynamics is better described by using larger values around 30 × 10^{21} s^{-1}. However, these conclusions contradict recent results obtained with sophisticated Langevin calculations, where the value of the dissipation parameter slightly decreases with deformation [17].

In order to contribute to this discussion, the SOFIA setup together with the inverse kinematics technique are used to obtain a complete characterization of both fission fragments produced via proton-induced fission on ^{208}Pb at kinetic energies of around 500A MeV [21]. These measurements were carried out using a thin liquid hydrogen target mounted inside a vacuum chamber. For the first time, the atomic and mass numbers of both fission fragments and their velocities were obtained simultaneously, defining new fission observables and correlations between them. In this work, these observables are utilized to investigate the magnitude and dependencies on temperature and deformation of the dissipation parameter.

Experiment

The experiment was carried out in the GSI facilities at Darmstadt (Germany), where the SIS18-synchrotron was utilized to accelerate heavy ions of ^{208}Pb at relativistic energies around 500*A* MeV. The ions were then guided to the experimental area *Cave C* to produce the fission reactions. Figure 1 shows a top-view schematic representation of the detector setup used in this experiment. The experimental setup is divided in two parts, one used to characterize the incoming beam ions and another dedicated to measure the fission fragments. The first part consists of a plastic scintillator detector (start) used to measure the time-of-flight (ToF) of the fragments, a multi-sampling ionization chamber (MUSIC) and a time projection chamber (TPC). These last two detectors provide the beam identification and its position on the target, respectively.

Fission measurements were then performed with a cylindrical target (11.24 mm long and 30 mm diameter) filled with liquid hydrogen with a thickness of (85.9 ± 1.5) mg/cm^2. A cryostat was used to liquefy the hydrogen and to keep it a constant pressure and temperature of around 1 atm and 20 K, respectively during the experiment [22]. The liquid hydrogen was isolated by two windows consisting of aluminized-mylar foils with a thickness of 35 μm. Finally, the cylindrical target was mounted inside a vacuum chamber in order to garantee that the fission reactions come only from the liquid hydrogen.

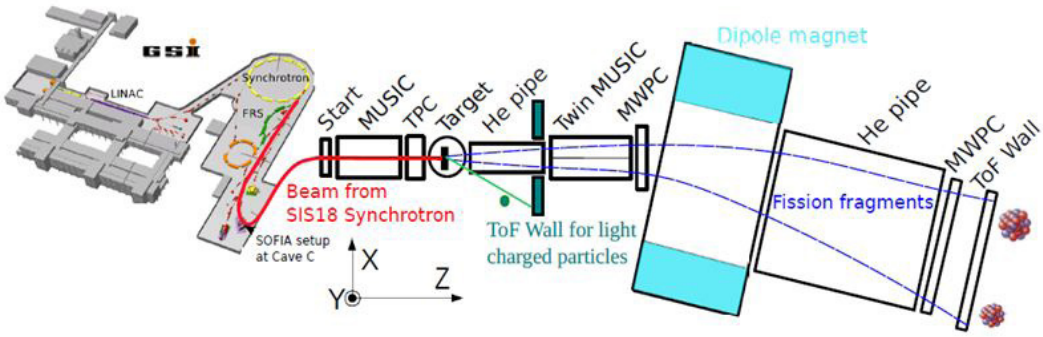

Figure 1: (Color online) Top schematic view of the experimental setup. Sizes are not to scale

The second part consists of a double multi-sampling ionization chamber (Twin MUSIC), two multiwire proportional counters (MWPCs), a large acceptance dipole magnet (ALADIN) and a ToF Wall. The Twin MUSIC chamber has a central vertical cathode that divides its volume into two active parts, segmented in ten anodes each. These anodes provide ten independent energy-loss and drift-time measurements, which allow to obtain the atomic numbers with a resolution below 0.43 charge units full width at half maximum (FWHM) and the angles on the plane *X*-*Z* with a resolution below 0.6 mrad (FWHM). MWPCs situated in front and behind the dipole magnet, provide the horizontal *(X)* and vertical *(Y)* positions of the fission fragments. The MWPC situated in front of the dipole magnet provides the *X* and *Y* positions with a resolution around 200 μm and 1.5 mm (FWHM), respectively, while the MWPC situated behind the dipole magnet provides those positions with a resolution around 300 μm and 2 mm (FWHM), respectively. A ToF Wall made of 28 plastic scintillators allows to measure the ToF of the fission fragments with respect to the start signal provided by the plastic scintillator located at the entrance of the experimental setup with a resolution around 40 ps (FWHM) [23]. The ALADIN magnet was set to a magnetic field of 1.6 T and its gap was filled with helium gas at atmospheric pressure. In addition, two pipes, also filled with helium gas at atmospheric pressure, were mounted in front of the Twin MUSIC chamber and behind the dipole magnet ALADIN. In all the cases, the helium gas was employed to reduce the energy and angular straggling of the fission fragments. The magnetic rigidity, velocity and atomic number of each fission fragment, together with a ray-tracing algorithm, were used to obtain its corresponding mass number *(A)* with an average resolution of A/A ~ 0.63% (FWHM).

Finally, light-charged particles (LCPs) emitted in coincidence with fission fragments were identified using a ToF wall detector (ToF of LCPs), placed in front the Twin MUSIC chamber. This detector consists of two detection planes of segmented plastic-

scintillators, one with six horizontal paddles and another with six vertical paddles, which leave a square whole (12.5 × 12.5 cm^2) in the center for the transmission of the fission fragments.

Results

These high-quality data allow obtaining fission observables sensitive to the ground-to-saddle and saddle-to-scission dynamics, which are compared with state-of-the-art model calculations to obtain information on dissipation. The code INCL was used to describe the first stage of the reaction between the proton and the nucleus as a series of independent hadron-hadron collisions, which leave an excited prefragment or compound nucleus [24-26]. The formed compound nucleus usually deexcites by emitting particles, and eventually fissioning. This last process is described by the deexcitation code ABLA07 which uses the Weisskopf formalism for the evaporation of particles, while the fission probability is determined by an analytical solution of the Fokker-Planck equation that includes a time-dependent correction. For the description of the saddle-to-scission dynamics we use the Hofmann-Nix formalism according to Ref. [27]. Other details can be found in Ref. [28].

The first observable used in this work is the sum of the charges of the final fission fragments Z_1+Z_2. This quantity is correlated with the impact parameter and thus with the initial excitation energy gained by the fissioning nucleus. The reason is that the excitation energy gained by the prefragments is strongly correlated with the number of knockout nucleons during the intranuclear cascade process. As shown in Ref. the average excitation energy of the fissioning system increases from 80 up to 350 MeV when decreasing Z_1+Z_2 [14]. The second observable is the width of the charge distribution of the final fission fragments (σ_Z), which is expected to strongly depend on the temperature of the system around the saddle point. Because the emission of protons after the saddle point is very improbable, the correlation between these two observables is used to investigate the fission dynamics at small de-formations. In addition, the width of the charge distribution depends on neither the entrance channel nor on the bombarding energy of the projectile [13,14]. This fact is shown in Figure 2(a), where this observable is displayed for the reaction ^{208}Pb + *p* at different kinetic energies. As can be seen, the width of the charge distribution is very similar for each fissioning system. The third observable used for the characterization of the fission process is the fission cross section. At low energies this quantity is strongly correlated with the height of the fission barrier. But at higher energies, the fission probability is also affected by the time needed for the transfer of energy between intrinsic and collective degrees of freedom. Because the fission cross sections are defined by the saddle point, this observable is also used to constrain the fission dynamics at small deformations.

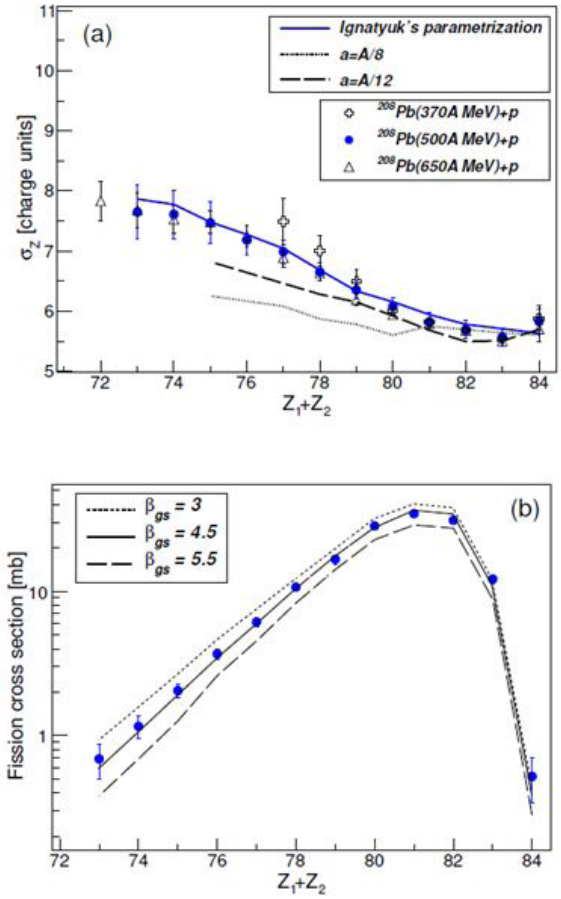

Figure 2: (Color online) Width of the atomic-number distribution of the fission fragments (a) and fission cross sections (b) as a function of the atomic number of the fissioning nuclei. The lines represent INCL4.6+ABLA07 calculations for different values of the level-density parameter and different values of the ground-to-saddle dissipation parameter β_{gs} in units of 10^{21} s^{-1}

Z1+Z2	σ [mb]	σZ [charge units]
84	0.52 ± 0.18	5.83 ± 0.21
83	12.13 ± 0.93	5.57 ± 0.15
82	30.98 ± 1.80	5.69 ± 0.14
81	34.45 ± 2.05	5.83 ± 0.15
80	28.34 ± 1.93	6.08 ± 0.16
79	16.66 ± 1.32	6.35 ± 0.16
78	10.69 ± 0.71	6.65 ± 0.18
77	6.14 ± 0.46	6.99 ± 0.20
76	3.68 ± 0.31	7.18 ± 0.25
75	2.05 ± 0.23	7.47 ± 0.35
74	1.16 ± 0.21	7.61 ± 0.40
73	0.69 ± 0.19	7.65 ± 0.45

Table 1: Partial fission cross sections (in mb) and width of the charge distributions for the different fissioning systems produced in the reaction ^{208}Pb + *p* at 500A MeV

Partial fission cross sections and widths of the charge distributions for the reaction ^{208}Pb + *p* at 500A MeV are listed in Table 1 together with their uncertainties, which are mainly due to statistical errors. These experimental data are also displayed in Figure 2(a) and 2(b) as a function of the atomic number of the fissioning system Z_1+Z_2. On the one hand, in Ref. [13] was demonstrated that the widths of the charge distributions are not sensitive to the value of the dissipation parameter. But assuming that the width of the charge distribution depends on the temperature at the saddle point, this observable should be sensitive to the value of the level-density parameter because it correlates the excitation energy with the temperature. In this sense, in Figure 2(a) we show model calculations considering different parametrizations of the level-density parameter. As can be seen, Ignatyuk's parametrization for the level-density parameter provides the best description (solid line), while the other parametrizations underestimate the data. On the other hand, in Figure 2(b) the fission cross sections are used to constrain the value of the ground-to-saddle dissipation parameter β_{gs}, taking into account that the level-density parameter was constrained in Figure 2(a). As can be seen, a value of 4.5×10^{21} s^{-1} (solid line) provides the best description of these data.

Finally, the last observable is the average neutron excess of the final fission fragments as a function of the fissioning system Z_1+Z_2 (Figure 3). This observable is affected by the neutron evaporation up to the scission point, and thus is sensitive to the ground-to-scission dynamics. However, as the presaddle dynamics was constrained by the use of the fission cross sections and the widths of the charge distributions of the fission fragments, this new observable can be utilized to study the value of the postsaddle dissipation parameter. The comparison of this observable with model calculations allows to determine the saddle-to-scission dissipation parameter β_{ss}, resulting in a value between 4.5 and 6.5 × 10^{21} s^{-1} [29].

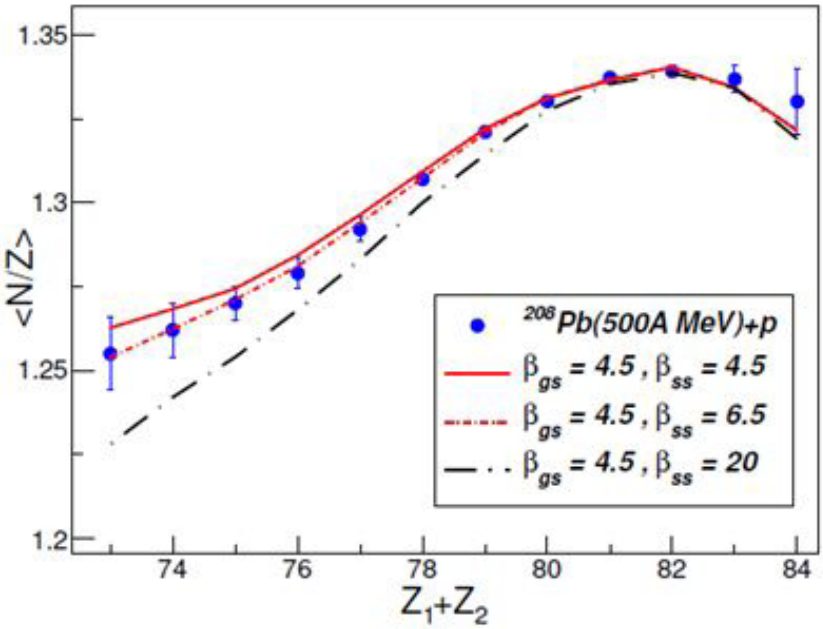

Figure 3: (Color online) Average neutron excess of the final fission fragments as a function of the atomic number of the fissioning nuclei. The lines represent model calculations for different values of the saddle-to-scission dissipation parameter β_{ss} in units of 10^{21} s^{-1}

Conclusion

Proton-induced fission reactions on ^{208}Pb at 500A MeV has been used to investigate the ground-to-scission fission dynamics. Fission cross sections and widths of the charge distributions of the fission fragments are utilized to constrain the ground-to-saddle dissipation parameter and the level-density parameter. The comparison allows concluding that a dissipation parameter of 4.5×10^{21} s^{-1} together with the parametrization proposed by Ignatyuk for the level-density parameter provide the best description of this set of data. Finally, the average neutron excess of the final fission fragments is used to constrain the saddle-to-scission dissipation parameter, obtaining a value between 4.5 and 6.5×10^{21} s^{-1}.

The similitude between the values of the dissipation parameter required to describe the fission dynamics before and after the saddle point excludes any strong dependence of this parameter with deformation. Moreover, the large range in excitation energy covered by the present data and their description by using a constant value of dissipation also exclude any strong dependence of this parameter with temperature. This work also confirms the need of using different independent observables to constrain the model parameters used in the description of the fission dynamics.

To go further, new experiments for the investigation of nuclear fission are planned at the GSI/FAIR facilities, in which quasi-free (p,2p) reactions are proposed as a novel tool to induce fission of heavy nuclei with high fissility like ^{238}U. As demonstrated in single-nucleon knockout reactions, this approach could allow determining the excitation energy of the fissioning system using complete kinematics measurements of the two outgoing protons, providing thus new constraints [30].

Acknowledgment

I would like to thank all the people who participated in the campaign of the SOFIA experiments at GSI and also the support from the Department of Education, Culture and University Organization of the Regional Government of Galicia under the program of postdoctoral fellowships.

References

1. Hinde DJ, Hilscher D, Rossner H, Gebauer B, Lehmann M, et al. (1992) Neutron emission as a probe of fusion-fission and quasifission dynamics. Phys Rev C 45: 1229.

2. Thoennessen M, Bertsch GF (1993) Threshold for dissipative fission. Phys Rev Lett 71: 4303.

3. Lestone JP (1993) Determination of the time evolution of fission from particle emission. Phys Rev Lett 70: 2245.

4. Ye W, Wang N (2013) Significant role of level-density parameters in probing nuclear dissipation with light-ion-induced fission excitation functions. Phys Rev C 87: 014610.

5. Moretto LG, Jing KX, Gatti R, Wozniak GJ, Schmitt RP (1995) Scaling Laws, Shell Effects, and Transient Times in Fission Probabilities. Phys Rev Lett 75: 4186.

6. Bohr N, Wheeler JA (1939) The Mechanism of Nuclear Fission. Phys Rev 56: 426.

7. Grangé P, Li Jun-Qing, Weidenmüller HA (1983) Induced nuclear fission viewed as a diffusion process: Transients Phys Rev C 27: 2063.

8. Fröbrich P, Gontchar II, Mavlitov ND (1993) Langevin fluctuation-dissipation dynamics of hot nuclei: Prescission neutron multiplicities and fission probabilities. Nucl Phys A 556: 281-306.

9. Schmitt C, Schmidt KH, Kelić A, Heinz A, Jurado B, et al. (2010) Fragmentation of spherical radioactive heavy nuclei as a novel probe of transient effects in fission Phys Rev C 81: 064602.

10. Jurado B, Schmitt C, Schmidt KH, Benlliure J, Enqvist T, et al. (2004) Transient Effects in Fission from New Experimental Signatures. Phys Rev Lett 93: 072501.

11. Jurado B, Schmidt KH, Benlliure J (2004) Time evolution of the fission-decay width under the influence of dissipation. Phys Lett B 553: 186-90.

12. Ayyad Y, Benlliure J, Casarejos E, Álvarez-Pol H, Bacquias A, et al. (2014) Proton-induced fission of ^{181}Ta at high excitation energies. Phys Rev C 89: 054610.

13. Ayyad Y, Benlliure J, Rodríguez-Sánchez JL, Bacquias A, Boudard A, et al. (2015) Dissipative effects in spallation-induced fission of ^{208}Pb at high excitation energies. Phys Rev C 91: 034601.

14. Rodríguez-Sánchez JL, Benlliure J, Taïeb J, Álvarez-Pol H, Audouin L, et al. (2015) Complete characterization of the fission fragments produced in reactions induced by ^{208}Pb projectiles on proton at 500A MeV Phys Rev C 91: 064616.

15. Fernández-García JP, Cubero M, Acosta L, Alcorta M, Alvarez MAG, et al. (2005) Simultaneous analysis of the elastic scattering and breakup channel for the reaction ^{11}Li+^{208}Pb at energies near the Coulomb barrier. Phys Rev C 92: 044612.

16. Rodríguez-Sánchez JL, Benlliure J, Paradela C, Ayyad Y, Casarejos E, et al. (2016) Light charged particles emitted in fission reactions induced by protons on ^{208}Pb. Phys Rev C 94: 034605.

17. Vardaci E, Nadtochy PN, Di Nitto A, Brondi A, La Ranaet G, et al. (2015) Fission dynamics of intermediate-fissility systems: A study within a stochastic three-dimensional approach. Phys Rev C 92: 034610.

18. Lestone JP, McCalla SG (2009) Statistical model of heavy-ion fusion-fission reactions. Phys Rev C 79: 044611.

19. Shaw NP, Diószegi I, Mazumdar I, Buda A, Morton CR, et al. (2000) Nuclear viscosity of hot rotating ^{240}Cf. J Phys Rev C 61: 044612.

20. Diószegi I, Shaw NP, Bracco A, Camera F, Tettoni S, et al. (2000) Fission hindrance in ^{200}Pb measured from giant dipole resonance γ-ray emission. Phys Rev C 63: 014611.

21. Martin JF, Taieb J, Chatillon A, Bélier G, Boutoux G, et al. (2015) Studies on fission with ALADIN. Eur Phys J A 51: 174.

22. Chesny P et al. (1996) GSI Annual Rep 97: 190.

23. Ebran A, Taieb J, Belier G, Chatillon A, Laurent B, et al. (2013) Picosecond resolution on relativistic heavy ions' time-of-flight measurement. Nucl Instr Meths A 728: 40-6.

24. Boudard A, Cugnon J, David JC, Leray S, Mancusi D (2013) New potentialities of the Liège intranuclear cascade model for reactions induced by nucleons and light charged particles. Phys Rev C 87: 014606.

25. Mancusi D, Boudard A, Cugnon J, David JC, Kaitaniemi P, et al. (2014) Extension of the Liège intranuclear-cascade model to reactions induced by light nuclei. Phys Rev C 90: 054602.

26. Rodríguez-Sánchez JL, David JC, Mancusi D, Boudard A, Cugnon J, et al. (2017) Improvement of one-nucleon removal and total reaction cross sections in the Liège intranuclear-cascade model using Hartree-Fock-Bogoliubov calculations. Phys Rev C 96: 054602.

27. Hofmann H, Nix JR (1983) Fission dynamics simplified. Phys Lett B 122: 117-20.

28. Kelic A, Ricciardi MV, Schmidt KH (2008) Proceedings of Joint ICTP-IAEA Advanced Work-shop on Model Codes for Spallation Reactions, ICTP Trieste, Italy, 4-8 February, pp. 181-221.

29. Rodríguez-Sánchez JL, Benlliure J, Taïeb J, Alvarez-Pol H, Audouin L, et al. (2016) Pre-saddle and post-saddle dissipative effects in fission using complete kinematics measurements. Phys Rev C 94: 061601(R).

30. Panin V, Taylor JT, Paschalis S, Wamers F, Aksyutina Y, et al. (2016) Exclusive measurements of quasi-free proton scattering reactions in inverse and complete kinematics. Phys Lett B 753: 204-10.